

## On the Reconstruction of Pointwise Power Distributions in a Fuel Assembly From Coarse-Mesh Nodal Calculations

Hun Young Jeong and Nam Zin Cho

Korea Advanced Institute of Science and Technology

(Received March 2, 1988)

노달계산결과로부터 핵연료 집합체내의 출력분포를 재생하는  
방법에 관하여

정훈영 · 조남진

한국과학기술원

(1988. 3. 2. 접수)

### Abstract

This paper is a study on an accurate and computationally efficient method for reconstructing pointwise power distributions from coarse-mesh nodal calculations. The modern nodal codes can calculate global reactor power shapes and criticality very efficiently and accurately. But inherent in the nodal procedures, there is inevitable loss of information on local heterogeneous quantities. In this study, an improved form function method which reflects the exponential transition of the thermal flux near the assembly surface is developed for the reconstruction of the heterogeneous fluxes. Use of the new form function method in several pressurized water reactor (PWR) benchmark problems reduces the maximum errors in the reconstructed thermal flux to those in the reconstructed fast flux. Even for assemblies adjacent to the steel baffle in realistic PWR cores, use of this method also results in improved pointwise power reconstruction.

### 요 약

현대 nodal code는 원자로의 출력분포와 임계도를 정확하면서도 매우 효율적으로 계산해 낸다. 그러나 이 경우 핵연료 집합체내의 세세한 출력분포는 알 수가 없게 되는데 본 논문에서는 이러한 것을 nodal 계산결과로부터 재생하는 방법에 대해서 연구해 보았다. 본 연구에서는 핵연료 집합체의 표면부근에서 열중성자속의 분포가 급격히 변하는 현상을 고려한 개선된 form function 방법을 개발하였다. 새 방법을 몇개의 가압경수로 benchmark problem에 응용해본 결과 기존의 방법에서 초래되었던 열 중성자속의 큰 재생오차가 속 중성자속의 재생오차와 비슷하게 줄었으며 따라서 출력분포의 재생오차도 크게 감소하였다. 또한 중성자속의 분포변화가 매우 큰 baffle과 인접한 집합체에서의 출력분포 재생오차도 크게 줄일 수 있었다.

## 1. Introduction

The neutronics design and safety analysis of a modern nuclear reactor require extensive knowledge of the power produced in the reactor core during both steady-state and transient operations. The ability to calculate power distributions in a nuclear reactor core depends critically on models used to predict the neutron density in space, direction, energy, and time. Fine-mesh finite difference methods for the neutron diffusion equation have been used for calculation of the power distributions in a reactor core.<sup>1)</sup> Unfortunately, because a large number of spatial mesh volumes are required for accurate solution of the finite-differenced diffusion equation, these methods are quite inefficient.

In the nodal methods, the reactor core is partitioned into large (typically, assembly size) homogeneous nodes, and as the unknowns, node averaged fluxes and surface averaged currents,<sup>2,3)</sup> and assembly average powers are directly obtained from the converged nodal solutions. Provided that accurate homogenized parameters which are generated from heterogeneous assembly calculations<sup>4)</sup> can be determined in a node, modern nodal codes are capable of accurately predicting global reactor power shapes, criticality, critical control rod patterns, etc. However, a major drawback of the nodal methods inherent in the homogenization procedures and the nodal scheme itself is the loss of information on local heterogeneous quantities.<sup>5)</sup> One is usually interested in local details at specific points or certain regions of the reactor, for instance, in the position and value of local pin power peaks in regions of high power density or detailed pin power distributions for some assemblies that are of particular interest.

Two basic approaches to the flux and power reconstruction from the nodal calculations were treated in the literature.<sup>5-9)</sup> These approaches are the imbedded assembly calculation method and the

approximate form function method. Although the imbedded assembly calculations can yield accurate reconstruction results, they are relatively expensive to implement, since they rely on auxiliary fine-mesh calculations for the node of interest. In the form function method, heterogeneous fluxes in each node are reconstructed by combining various modes of form functions with the assembly heterogeneous flux which is saved from the assembly calculation. The nineterm bi-quadratic form function method<sup>7,8)</sup> is most satisfactory of all form function methods from a point of view of accuracy and efficiency. However, this method approximates flux distributions poorly in an assembly-size node, specially thermal flux. In determining pointwise power distributions, it is important to reconstruct thermal flux more accurately than fast flux, since most fission power in a thermal reactor is produced by thermal fissions.

In this paper, efficient form function methods are investigated for the pointwise power reconstruction. An improved form function method<sup>10)</sup> whose reconstruction error of the thermal flux is roughly that of the fast flux is described, and its reconstruction results are compared with those of the bi-quadratic form function method.

## 2. Modern Nodal Theory and Equivalent Assembly Homogenization

### 2.1. Modern Nodal Theory

It is assumed that two-group cross sections are spatially constant in each node and that the values of these constants are provided by the methods described in the next section. Then, the three-dimensional static multigroup neutron diffusion equation is

$$\nabla \cdot \vec{J}_g^{\text{hom}}(\vec{r}) + \Sigma_{tg}(\vec{r}) \phi_g^{\text{hom}}(\vec{r}) = \sum_{g'=1}^{G-1} [\Sigma_{gg'}(\vec{r}) + \frac{\chi_{gg'}}{k_{\text{eff}}} \nu \bar{\Sigma}_{f g'}(\vec{r})] \phi_{g'}^{\text{hom}}(\vec{r}) \quad (2.1)$$

$$\vec{J}_g^{\text{hom}}(\vec{r}) = -\bar{D}_g(\vec{r}) \nabla \cdot \phi_g^{\text{hom}}(\vec{r}); \quad (2.2)$$

$$g=1,\dots,G.$$

Integration of equation (2-1) over the volume of node  $N(N=1,\dots,N_{core})$  yields

$$\begin{aligned} & h_y^N h_z^N [\bar{J}_{gN}^{x,hom}(x_{i+1}) - \bar{J}_{gN}^{x,hom}(x_i)] \\ & + h_z^N h_x^N [\bar{J}_{gN}^{y,hom}(y_{i+1}) - \bar{J}_{gN}^{y,hom}(y_i)] \\ & + h_x^N h_y^N [\bar{J}_{gN}^{z,hom}(z_{k+1}) - \bar{J}_{gN}^{z,hom}(z_k)] \\ & + V^N \sum_{lgN} \bar{\phi}_{gN}^{hom} = V^N \sum_{g=1}^G [\bar{\Sigma}_{gg'N} \\ & + \frac{x_g}{k_{eff}} \nu \bar{\Sigma}_{lg'N}] \bar{\phi}_{gN}^{hom} \end{aligned} \quad (2.3)$$

where

$$\begin{aligned} \bar{J}_{gN}^{u,hom}(ul) &= \frac{1}{h_v^N h_w^N} \int_{v_m}^{v_{m+1}} dv \\ & \int_{w_n}^{w_{n+1}} dw \bar{J}_g^{hom}(ul, v, w); \\ & u=x, y, z, \quad w \neq v \neq u \\ & l=i, j, k \quad l \neq m \neq n \\ \bar{\Sigma}_{\alpha gN} &= \sum_{\alpha g} \Sigma_{\alpha g}(x, y, z) \mid x \in [x_i, x_{i+1}] \\ & \mid y \in [y_i, y_{i+1}] \\ & \mid z \in [z_k, z_{k+1}]; \quad \alpha = t, a, gg', f \end{aligned}$$

$$\bar{\phi}_{gN}^{hom} = \frac{1}{V^N} \int_{V^N} dV \phi_g^{hom}(\vec{r})$$

$$\begin{aligned} V^N &= h_x^N h_y^N h_z^N; h_x^N = x_{i+1} - x_i \\ h_y^N &= y_{i+1} - y_i, \quad h_z^N = z_{k+1} - z_k. \end{aligned}$$

Equation (2-3) is called the nodal balance equation. The utility of this equation is limited by the fact that without additional relationships between the face-averaged currents  $\bar{J}_{gN}^{u,hom}(ul)$  and the node-averaged fluxes  $\bar{\phi}_{gN}^{hom}$  the spatial flux distribution cannot be determined. The required relationships are called the spatial coupling equations, and in the modern nodal theory these equations are derived by integrating the diffusion equation over the directions transverse to the direction of interest. This yields for the direction  $u(=x,y,z)$  and node  $N$ ,

$$-\bar{D}_{gN} \frac{\partial^2}{\partial u^2} \bar{\phi}_{gN}^{u,hom}(u) + \bar{\Sigma}_{lgN} \bar{\phi}_{gN}^{u,hom}(u)$$

$$- \sum_{g'=1}^G [\bar{\Sigma}_{gg'N} + \frac{x_g}{k_{eff}} \nu \bar{\Sigma}_{fg'N}] \bar{\phi}_{g'N}^{u,hom}(u)$$

$$= -S_{gN}^u(u) \quad (2.4)$$

where

$$\begin{aligned} \bar{\phi}_{gN}^{u,hom}(u) &= \frac{1}{h^N h_w^N} \int_{v_m}^{v_{m+1}} dv \\ & \int_{w_n}^{w_{n+1}} dw \phi_g^{hom}(u, v, w) \end{aligned}$$

is the one-dimensional flux in group  $g$  and in direction  $u$  for node  $N$ , and

$$\begin{aligned} S_{gN}^u(\bar{u}) &= -\frac{\bar{D}_{gN}}{h_v^N h_w^N} \int_{v_m}^{v_{m+1}} dv \int_{w_n}^{w_{n+1}} dw \\ & \frac{\partial^2}{\partial u^2} \phi_g^{hom}(u, v, w) - \frac{\bar{D}_{gN}}{h_y^N h_w^N} \int_{v_m}^{v_{m+1}} dv \\ & \int_{w_n}^{w_{n+1}} dw \frac{\partial^2}{\partial w^2} \phi_g^{hom}(u, v, w) \end{aligned} \quad (2.5)$$

is called the transverse leakage term which represents the neutron leakage transverse to the direction  $u$ .

Note that

$$\frac{1}{h_u^N} \int_{ul}^{ul+1} du \bar{\phi}_{gN}^{u,hom}(u) = \bar{\phi}_{gN}^{hom}(u) \quad (2.6)$$

$$-\bar{D}_{gN} \frac{\partial}{\partial u} \bar{\phi}_{gN}^{u,hom}(u) \Big|_{u=ul} = \bar{J}_{gN}^{u,hom}(ul) \quad (2.7)$$

Thus, if the one-dimensional flux  $\bar{\phi}_{gN}^{u,hom}(u)$  is known, the relationships between the node-averaged fluxes and the surface-averaged currents can be obtained. Various modern nodal methods are distinguished from one another by the way to treat the spatial coupling equations. In this study, the ANM nodal code<sup>(11)</sup> which is based on the analytic nodal method<sup>(12)</sup> is used in order to obtain nodal solutions.

## 2.2. Equivalent Assembly Homogenization

In order to apply nodal methods to reactor analysis, the heterogeneous assemblies must be homogenized. The most commonly used proce-

ture to determine the homogenized parameters in each assembly is the assembly calculation method. In this method, a relatively inexpensive heterogeneous assembly eigenvalue calculation is performed using the zero-net-current boundary condition to yield a heterogeneous assembly flux  $A_g(\vec{r})$  for each unique type of assemblies. Then the conventional flux-volume weighting method is applied with this heterogeneous assembly flux:

$$\bar{\Sigma}_{a,gN} = \frac{\int_{V_N} dV \Sigma_{a,g}(\vec{r}) A_g(\vec{r})}{\int_{V_N} dV A_g(\vec{r})} \quad (2.8)$$

$$\bar{D} = \frac{\int_{V_N} dV D_g(\vec{r}) A_g(\vec{r})}{\int_{V_N} dV A_g(\vec{r})} \quad (2.9)$$

These assembly homogenized parameters are designated as assembly homogenized cross sections (AXS). Smith<sup>4)</sup> introduced discontinuity factors in order to correct the discontinuity of the surface-averaged homogeneous flux at the node interface. Smith's assembly discontinuity factors (ADF) are

$$ADF_{gN}^{u+} = \frac{\bar{A}_{gN}^u(u_{l+1})}{\bar{A}_{gN}^{u,hom}(u_{l+1})} \quad (2.10)$$

$$ADF_{gN}^{u-} = \frac{\bar{A}_{gN}^u(u_l)}{\bar{A}_{gN}^{u,hom}(u_l)} \quad (2.11)$$

Then continuity condition for the heterogeneous surface-averaged flux is expressed as

$$ADF_{gN}^{u+} \cdot A_{gN}^{u,hom}(u_{l+1}) = ADF_{gK}^{u-} \cdot A_{gK}^{u,hom}(u_l)$$

where the  $u+$  surface of the node  $N$  is corresponds to the  $u$ -surface of the node  $K$ . The homogeneous flux from a homogeneous assembly calculation with the zero-net-current boundary condition is spatially flat and thus

$$\bar{A}_{gN}^{u,hom}(u_l) = \bar{A}_{gN}^{u,hom}(u_{l+1}) = \bar{A}_{gN}^{hom} = \bar{A}_{gN}$$

where  $\bar{A}_{gN}^{hom}$  and  $\bar{A}_{gN}$  are the assembly-volume averages of the homogeneous and heterogeneous assembly fluxes, respectively. Thus, when assembly calculations are based on zero-net-current

boundary conditions, the ADF can also be expressed as

$$ADF_{gN}^{u+} = \frac{\bar{A}_{gN}^u(u_{l+1})}{\bar{A}_{gN}} \quad (2.12)$$

$$ADF_{gN}^{u-} = \frac{\bar{A}_{gN}^u(u_l)}{\bar{A}_{gN}} \quad (2.13)$$

### 3. Reconstruction of Pointwise Power Distributions

The reconstruction of heterogeneous fluxes and power distributions from the nodal solution is especially appealing because these detailed distributions can be obtained separately from the evaluation of global and node-averaged quantities. The detailed information is computed only when and where desired,<sup>5)</sup> after nodal calculations are executed.

So far two independent methods have been developed for the reconstruction problem. The more accurate and expensive method of these two is the imbedded heterogeneous assembly calculation method.<sup>5,6)</sup> Basic approach to this method is to derive accurate boundary conditions at the node surfaces directly from the converged nodal solution and then to solve an assembly source problem with these boundary conditions. The second approach to flux reconstruction is the various form function methods, including the modulation method,<sup>5)</sup> FORTE method,<sup>7)</sup> and bi-quadratic form function method.<sup>8)</sup> The essence of the form function methods is to search for a form function,  $F_g(x,y)$ , that multiplicatively corrects the assembly flux,  $A_g(x,y)$ , such that the product  $A_g(x,y)XF_g(x,y)$  reconstructs the heterogeneous flux,  $\phi_g(x,y)$ , within an assembly:

$$\phi_g(x,y) = A_g(x,y)XF_g(x,y). \quad (3.1)$$

That is, the assembly flux reflects local heterogeneities within an assembly and the form function represents smooth flux distribution in the

global core. In contrast to the imbedded assembly calculation method, since the  $A_g(x,y)$  are needed in the first place to determine the homogenized nodal parameters, reconstruction can be performed at a little additional cost without any auxiliary fine-mesh calculation. Because of its greater computational efficiency, only the form function methods are investigated in this paper.

### 3.1. Bi-quadratic Form Function Method

In this method, the form function of the group flux is approximated by a nine-term bi-quadratic polynomial, i.e.,

$$F_g(x,y) = \frac{\phi_g(x,y)}{A_g(x,y)} \sim \sum_{m=0}^2 \sum_{n=0}^2 a_{m,ng} \left(\frac{x}{h_x}\right)^m \left(\frac{y}{h_y}\right)^n \quad (3.2)$$

The nine coefficients  $a_{m,ng}$  for each group are determined by the requirement that the reconstructed flux  $\phi_g(x,y) = A_g(x,y)XF_g(x,y)$  yield the correct values of the nine flux-related quantities:

- i) The node-volume averaged flux,
- ii) The node-surface averaged fluxes,  $s=1,\dots,4$ ,
- iii) The corner-point fluxes,  $c=1,\dots,4$ .

Here the corner-point fluxes are interpolated values by using the node-surface averaged fluxes. In this paper, the CAMPANA method<sup>7)</sup> is adopted for the corner-point flux interpolation. Fig. 1 illustrates the coordinate system and the various flux information used to evaluate the  $a_{m,ng}$ . The requirements that  $A_g(x,y)XF_g(x,y)$  match the nine flux values are as follows.

$$\phi_g = \frac{1}{h_x h_y} \int_0^{h_y} dy \int_0^{h_x} dx A_g(x,y) \cdot F_g(x,y), \quad (3.3)$$

$$\phi_g^1 = \frac{1}{h_y} \int_0^{h_y} dy A_g(0,y) \cdot F_g(0,y), \quad (3.4)$$

$$\phi_g^2 = \frac{1}{h_y} \int_0^{h_y} dy A_g(h_x,y) \cdot F_g(h_x,y), \quad (3.5)$$

$$\phi_g^3 = \frac{1}{h_x} \int_0^{h_x} dx A_g(x,0) \cdot F_g(x,0), \quad (3.6)$$

$$\phi_g^4 = \frac{1}{h_x} \int_0^{h_x} dx A_g(x,h_y) \cdot F_g(x,h_y), \quad (3.7)$$

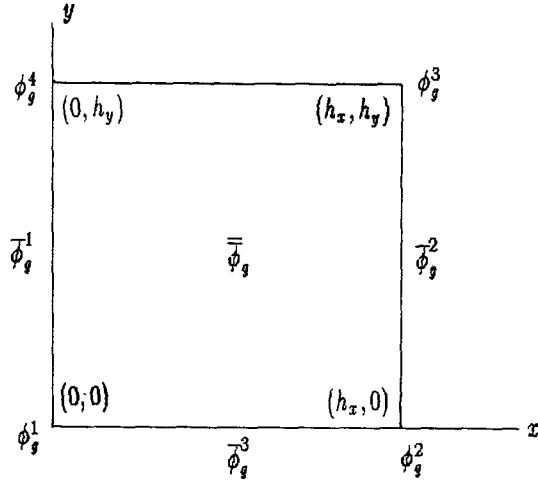


Fig. 1. Coordinate System and Flux Information Used for Flux Reconstruction

$$\phi_g^1 = A_g(0,0) \cdot F_g(0,0) \quad (3.8)$$

$$\phi_g^2 = A_g(h_x,0) \cdot F_g(h_x,0) \quad (3.9)$$

$$\phi_g^3 = A_g(h_x,h_y) \cdot F_g(h_x,h_y) \quad (3.10)$$

$$\phi_g^4 = A_g(0,h_y) \cdot F_g(0,h_y) \quad (3.11)$$

Equations (3.3) through (3.11) can be written in matrix form as

$$[B_g][a_{m,ng}] = [\phi_g] \quad (3.12)$$

and this system of equations can easily be solved directly.

### 3.2. Improved Form Function Method

Applications of the bi-quadratic form function method to heterogeneous flux reconstruction show that although reconstruction results of the fast flux are satisfactory, results of the thermal flux are not as good as those of the fast flux.<sup>7)</sup> These results imply that the form function for the fast flux is well fitted by a polynomial function, but not for the thermal flux.

This is explained as follows. The slowing down density of the fast neutrons in the interior of a homogeneous medium is proportional to the fast

neutron density,<sup>13)</sup> and thus the thermal neutron flux is proportional to the fast neutron flux. But near the interface of the distinct types of material, the neutron spectrum is affected by the material and spectral interaction. Because the mean free path of the thermal neutrons is very short and that of the fast neutrons is relatively long, comparable to the assembly size, the thermal neutron flux distributions may change drastically while the fast neutron distributions may not. Therefore, the ratio of the thermal flux to the fast flux would show exponential transitions near the assembly interface.

Based on the Koebke's spectral interpolation scheme<sup>9)</sup> for a homogeneous reactor, an improved form function method is developed in this study for the reconstruction of the heterogeneous flux. In this method, the bi-quadratic form function method is adopted for the reconstruction of the fast flux,

$$F_1(x,y) = \sum_{m=0}^2 \sum_{n=0}^2 a_{m,n} \left(\frac{x}{h_x}\right)^m \left(\frac{y}{h_y}\right)^n, \quad (3.13)$$

while for the reconstruction of the thermal flux, a group dependent form function is used in the following form

$$\frac{F_2(x,y)}{F_1(x,y)} = \sum_{i=0}^2 \sum_{j=0}^2 c_{ij} G_i(x) G_j(y) \quad (3.14)$$

where

$$G_0(t) = 1$$

$$G_1(t) = \cosh\left(\frac{t}{L_2}\right)$$

$$G_2(t) = \sinh\left(\frac{t}{L_2}\right), \quad t=x,y$$

and

$$L_2 = \sqrt{\frac{\bar{D}_2}{\bar{\Sigma}_{a2}}}$$

Here  $\bar{D}$  and  $\bar{\Sigma}_{a2}$  are homogenized values. If  $F_1(x,y)$  is precalculated, the nine coefficients of

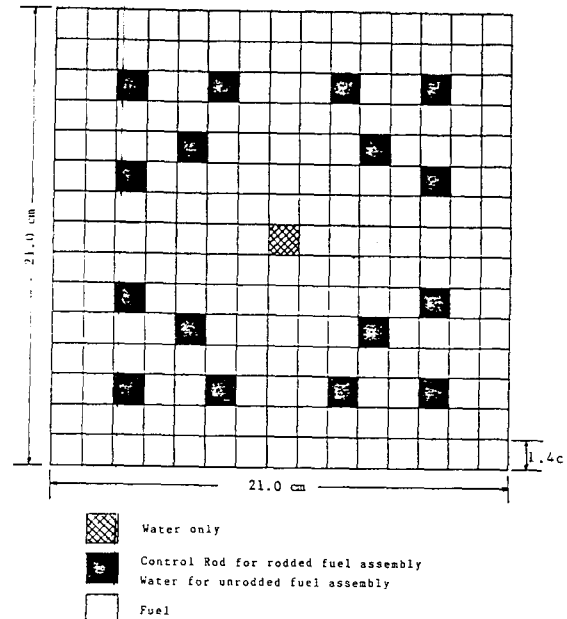


Fig. 2. Heterogeneous PWR Assembly Geometry

$F_2(x,y)$  can be determined by the previous procedure, Eq. (3.3) through Eq. (3.12), and then the thermal flux is reconstructed as

$$\phi_2(x,y) = A_2(x,y) \cdot F_1(x,y) \left[ \sum_{i=0}^2 \sum_{j=0}^2 c_{ij} G_i(x) G_j(y) \right].$$

#### 4. Applications and Discussions

The accuracy of the new form function method for pointwise flux and power reconstruction is tested on several PWR benchmark problems described in Figures 2 through 5 and Table 1. All reconstruction results are compared with those of the bi-quadratic form function method. For this purpose, ANM calculations using AXS/ADF were performed with 2X2 nodes per assembly. However, reconstruction of the pointwise quantities was over one node per assembly, since an objective of this study is to develop an efficient reconstruction scheme with one node per assembly. Since the difference between the bi-quadratic form function method and the new form function method developed in this study is only the reconstruction scheme for the thermal flux, pointwise thermal

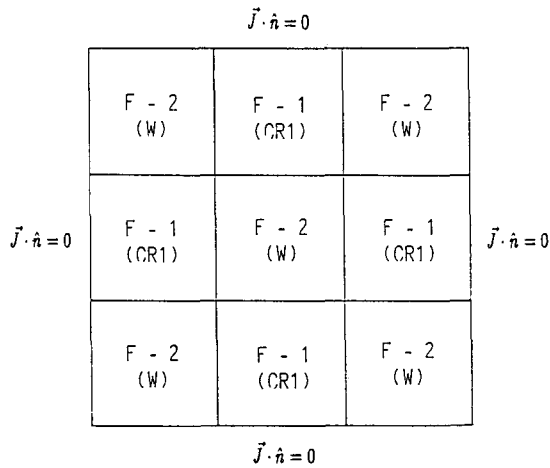


Fig. 3. Benchmark Problem 1

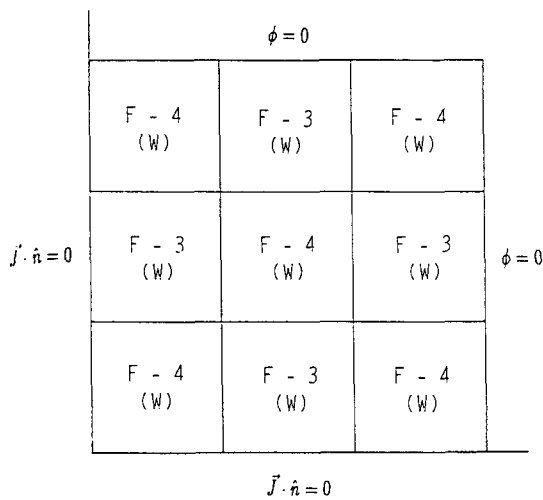


Fig. 4. Benchmark Problem 2

flux reconstruction results are compared at first and then pointwise power reconstruction results are presented. The pointwise power is obtained as

$$P(x,y) = \sum_{g=1}^2 k \sum_{fg} f_{fg}(x,y) \phi_g(x,y)$$

where  $k(=3.3 \times 10^{-11} \text{ Ws})$  is energy release per fission. The global reference solutions are from the fine-mesh (2X2 mesh per each pin-cell, i.e., a mesh size of 0.7 cm) KIDD<sup>14)</sup> runs.

Table 2 presents the flux and power reconstruction results for the center node of Benchmark Problems 1 and 2. Benchmark Problem 1 is de-

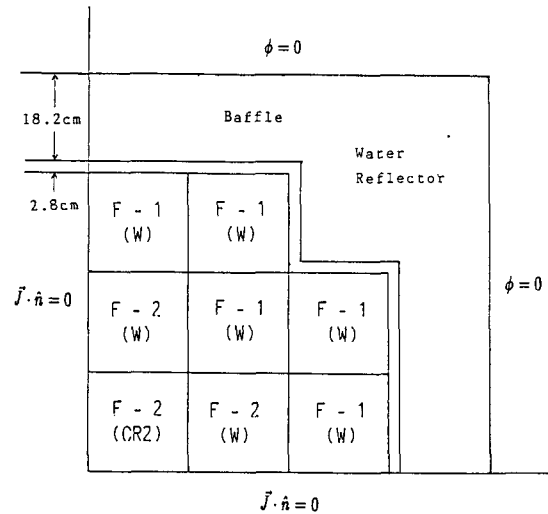


Fig. 5. Benchmark Problem 3

signed to simulate the reactor core containing control rods, and Benchmark Problem 2 is designed to represent the effect of flux tilt. Table 2 shows that when the bi-quadratic form function method is used for the reconstruction, the reconstruction results for the fast flux are good but not for the thermal flux and the pointwise power. On the other hand, when the new method is used, we get significantly improved reconstruction results. In the new method, the error of the reconstructed thermal flux and pointwise power is similar to that of the reconstructed fast flux.

The new reconstruction method is also tested with Benchmark Problem 3 which is a more realistic PWR problem. This problem contains a rodged assembly, steel-baffle, and water reflector. Reconstruction results for Benchmark Problem 3 are presented in Figs. 6 and 7. In this problem, relatively large errors arise in the rodged assembly and assemblies adjacent to the steel-baffle. For the rodged assembly, somewhat unsatisfactory results are mainly from the irregular flux distributions in the interior of the assembly caused by control rods. For assemblies adjacent to the baffle, the maximum error in reconstruction of the thermal flux is -17.3% with the bi-quadratic method. This large error is due to the steel-baffle and water

**Table 1. Heterogeneous, Pin-cell Two-group Cross Section Data for Benchmark Problems**

Cross-Section	g	Fuel 1	Fuel 2	Fuel 3	Fuel 4	Control Rod 1	Control Rod 2	Water	Steel Baffle
$D_g$ (cm)	1	1.500	1.500	1.500	1.500	1.1133	1.1133	1.700	1.020
	2	0.400	0.400	0.400	0.400	0.18401	0.18401	0.350	0.335
$\Sigma_{gg'}$ ( $cm^{-1}$ )	1	0.020	0.020	0.020	0.020	0.037529	0.0037529	0.035	0.0
	2	0.0	0.0	0.0	0.0	0.0	0.0	0.0	0.0
$\Sigma_{ag}$ ( $cm^{-1}$ )	1	0.013	0.010	0.010	0.011	0.049890	0.0836661	0.001	0.00322
	2	0.180	0.15	0.160	0.190	0.96726	0.96726	0.05	0.146
$\nu \Sigma_{fg}$ ( $cm^{-1}$ )	1	0.0065	0.005	0.0065	0.0055	0.0	0.0	0.0	0.0
	2	0.240	0.180	0.240	0.2100	0.0	0.0	0.0	0.0
$k \Sigma_{fg}$ (Ws/cm)	1	8.850E-14	6.600E-14	8.850E-14	7.260E-14	0.0	0.0	0.0	0.0
	2	3.168E-12	2.376E-12	3.168E-12	2.772E-12	0.0	0.0	0.0	0.0

**Table 2. Reconstruction Results for The Center Node of Benchmark Problems 1 and 2**

	Benchmark Problem	Method	Average Error	Maximum Error
Fast Flux	1	Bi-quadratic	0.25%	0.92%
	2	Bi-quadratic	0.53%	-2.01%
Thermal Flux	1	Bi-quadatic	2.88%	8.13%
		New	0.47%	1.50%
	2	Bi-quadratic	2.57%	-8.32%
		New	0.59%	-1.70%
Power	1	Bi-quadratic	2.49%	7.09%
		New	0.43%	1.67%
	2	Bi-quadratic	2.17%	-7.02%
		New	0.57%	-1.75%

Note: Pointwise error at(i,j) =  $E_{i,j} = (cal.-ref.)/ref. \times 100\%$

Maximum error =  $\text{Max}(E_{i,j})$

Average error =  $\sum |E_{i,j}| / \text{Total number of points}$

reflector. On approaching the steel-baffle, the thermal flux changes rapidly. Thus the bi-quadratic method cannot represent this effect adequately, resulting in large errors. In applying the new method, these large errors are reduced to 8.9% from -17.3% in the thermal flux reconstruction and to 7.0% from -14.2% in the pointwise power reconstruction.

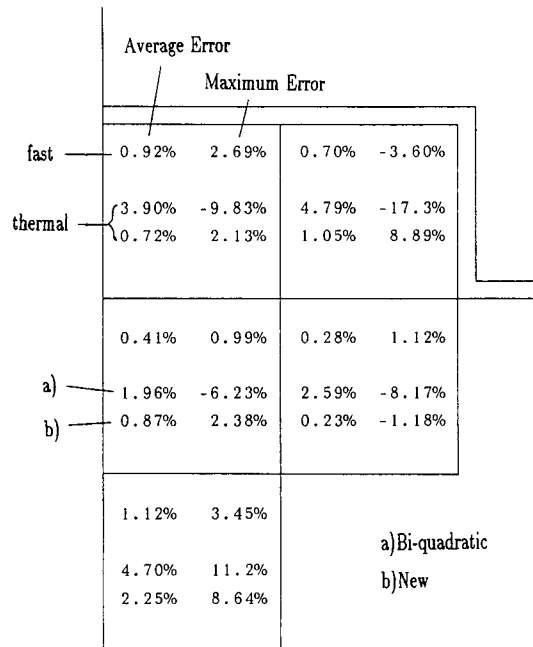


**Fig. 6. Pointwise Flux Reconstruction Results for Benchmark Problem 3**

**5. Summary**

An improved form function method for reconstruction of pointwise flux and power from coarse-mesh nodal calculations has been developed in this study. In contrast to the conven-



	Average Error		Maximum Error	
a)	3.03%	-7.67%	3.85%	-14.2%
b)	0.72%	2.13%	0.92%	6.96%
	1.62%	-5.23%	2.07%	-6.32%
	0.77%	2.01%	0.23%	-0.73%
	3.88%	9.16%	a) Bi-quadratic b) New	
	1.97%	7.29%		

**Fig. 7. Pointwise Power Reconstruction Results for Benchmark Problem 3**

tional polynomial form function method, the new method uses hyperbolic form function for the thermal flux to represent exponential transition behavior near the assembly interface and treats the form function of the thermal flux not independently of the form function of the fast flux. The new method led to large error reduction in the reconstructed thermal flux, and showed similar error reduction in the reconstructed pointwise power. Thus the new form function method is able to reconstruct all heterogeneous quantities efficiently and satisfactorily, provided that accurate coarse-mesh nodal solutions are obtained.

**Acknowledgements**

We like to express gratitude to Messrs. Kap Suk Moon, Jae Man Noh, and Il-Seop Jung of the Reactor Core Design Group at Korea Advanced Energy Research Institute for generously allowing

us to use their computing facilities and for their valuable help during the course of the work.

**References**

1. C. H. Adams, "Current Trends in Methods for Neutron Diffusion Calculations," Nucl. Sci. Eng., 64, 552, 1977.
2. A. F. Henry, "Refinements in Accuracy of Coarse-Mesh Finite Difference Solution of the Group Diffusion Equations," in Nuclear Reactor Calculations, p. 447, IAEA, Vienna, 1972.
3. R. D. Lawrence, "Progress in Nodal Methods for the Solution of the Neutron Diffusion and Transport Equations," Prog. Nucl. Energy, 17, 271, 1985.
4. K. S. Smith, "Assembly Homogenization Techniques for Light Water Reactor Analysis," Prog. Nucl. Energy, 17, 303, 1985.
5. K. Koebke and M. R. Wagner, "The Determination of Pin Power Distribution in a Reactor Core on The Basis of Nodal Coarse Mesh Calculations," Atomkernenergie, 30, 136, 1977.
6. A. Jonsson, S. Grill, and R. Rec, "Nodal Imbedded Calculation for the Retrieval of Local Power Peaking From Coarse Mesh Reactor Analysis," Proc. of the International Topical Meeting on Advances in Mathematical Methods for the Solution of Nuclear Engineering Problems, Munich, W. Germany, Vol. 2, pp. 23-41, April 1981.
7. C. L. Hoxie, "Application of Nodal Equivalence Theory to the Neutronics Analysis of PWR's," Ph. D. Thesis, Department of Nuclear Engineering, M. I. T., Cambridge, MA, June 1982.
8. K. S. Khalil, "The Application of Nodal Methods to PWR Analysis," Ph. D. Thesis, Department of Nuclear Engineering, M. I. T., Cambridge, MA, January 1983.
9. K. Koebke and L. Hetzelt, "On The Reconstruction of Local Homogeneous Neutron Flux and Current Distributions of Light Water Reactors From Nodal Schemes," Nucl. Sci. Eng., 91, 123, 1985.
10. H. Y. Jeong, "The Reconstruction of Pointwise Power Distributions in a Light Water Reactor Core From Coarse-Mesh Nodal Calculations," M. S. Thesis, Department of Nuclear Engineering, Korea Advanced Institute of Science and Technology, December 1987.
11. J. Chang, K. S. Moon, and M. H. Kim, "ANM: Coarse-mesh Nodal Code Based on Analytic Nodal

- Method," Korea Advanced Energy Research Institute (to be published).
12. K. S. Smith, "An Analytic Nodal Method for Solving the Two-group, Multidimensional, Static and Transient Neutron Diffusion Equation," Nuclear Engineer's Thesis, Department of Nuclear Engineering, M. I. T., Cambridge, MA, 1979.
  13. J. R. Lamarsh, Introduction to Nuclear Reactor Theory, Addison-Wesley, Reading, Mass., 1966.
  14. S. K. Lee, K. S. Moon, J. Chang, and B. J. Jun, "KIDD-KAERI Improved Diffusion Depletion Program for Nuclear Reactor Analysis," Korea Advanced Energy Research Institute (to be published).